JOURNAL OF MATERIALS SCIENCE **38** (2003) 4259–4270

Doping and defect association in oxides for use in oxygen sensors

J. W. FERGUS
Auburn University, Materials Research and Education Center, 201 Ross Hall, Auburn, AL 36849, USA
E-mail: jwfergus@eng.auburn.edu

Oxygen sensors provide valuable information for improving the efficiency of, and thus reducing harmful emissions from, combustion processes, such as in internal combustion engines. Oxide materials can be used in different ways to generate an oxygen partial pressure dependent output. The type of sensor in which a particular oxide is used depends on the ionic and electronic defects in the oxide, which can be, to some extent, controlled by doping. In this paper, the issues in selection of an oxide for use in resistive-type, potentiometric-type and amperometric-type oxygen sensors are reviewed. Prototypical examples of materials, specifically titania and zirconia, commonly used in these sensors are discussed to illustrate the effects of doping and defect interaction on the electrolytic and transport properties of oxide materials for use in oxygen sensors.

1. Introduction

Industrial processes and products contain increasing numbers of sensors for improved efficiency and performance. For example, among the wide variety of sensors for improved safety and performance in automobiles [1, 2], chemical sensors are used to improve the operating efficiency and reduce emissions of the internal combustion engine [3, 4]. Sensors are being developed to measure various exhaust emissions, such as CO [5–9], NO_x [8–11], hydrocarbon gases [5, 6, 11] and hydrogen [6, 12]. However, the most widely used sensor is the exhaust gas oxygen (EGO) sensor, the output of which is used to control the air-to-fuel ratio for improved engine efficiency [13, 14]. Similar oxygen sensors are used in other combustion processes [15], including wood burning [16].

2. Types of oxygen sensors

Three different ways in which oxides are used in oxygen sensors are shown schematically in Fig. 1 [17–20]. In all cases, the output of the sensor relies on reactions between defects in the oxide and oxygen in the atmosphere. If the predominant defect is an oxygen vacancy ($V_O^{\bullet\bullet}$), this equilibrium can be described by Reaction 1,

$$\frac{1}{2}O_2 + V_O^{\bullet\bullet} + 2e' = O_O^x \qquad (1)$$

where the ions and defects in the solid are represented using Kröger-Vink notation [21].

Resistive-type sensors (Fig. 1a) use the relationship between the concentrations of ionic and electronic defects in the oxide and the partial pressure of oxygen in the atmosphere to produce the sensor output. For example, in an *n*-type semiconducting material, if the oxygen partial pressure increases, Reaction 1 will proceed in the forward direction, which will result in a decrease in the concentrations of oxygen vacancies and electrons, and thus a decrease in conductivity. The electrical resistance of such a semiconducting oxide is related to the oxygen partial pressure in the surrounding atmosphere, and thus can be used as the sensor output.

Potentiometric- and amperometric-type sensors, on the other hand, use oxides that are solid electrolytes, where the ionic transport number (t_{ion}), which is the ionic conductivity divided by the total conductivity, is greater than 0.99, so that electronic conduction (electrons or holes) makes only a small contribution (typically less than 1%) to the total conductivity. In potentiometric-type oxygen sensors (Fig. 1b), two electrodes (reference and sensing) are separated by a solid electrolyte. The difference between the oxygen partial pressure at the reference electrode ($P_{O_2}^{reference}$) and that at the sensing electrode ($P_{O_2}^{sensing}$) generates a voltage (E) according to the Nernst equation,

$$E = (t_{O^{2-}}) \cdot \left(\frac{RT}{4F}\right) \cdot \ln\left(\frac{P_{O_2}^{sensing}}{P_{O_2}^{reference}}\right) \qquad (2)$$

where R is the gas constant, T is absolute temperature, F is Faraday's constant and $t_{O^{2-}}$ is the transport number for oxide ions, which is equal to one for a solid electrolyte. A potentiometric sensor operates under open-circuit conditions, where no electrical current flows through the external electrical current, which prevents ionic current from flowing through the electrolyte. If the electrolyte material were not a pure ionic conductor, electrical current could flow through the electrolyte, even in open-circuit conditions, which would lead to an erroneously low output voltage.

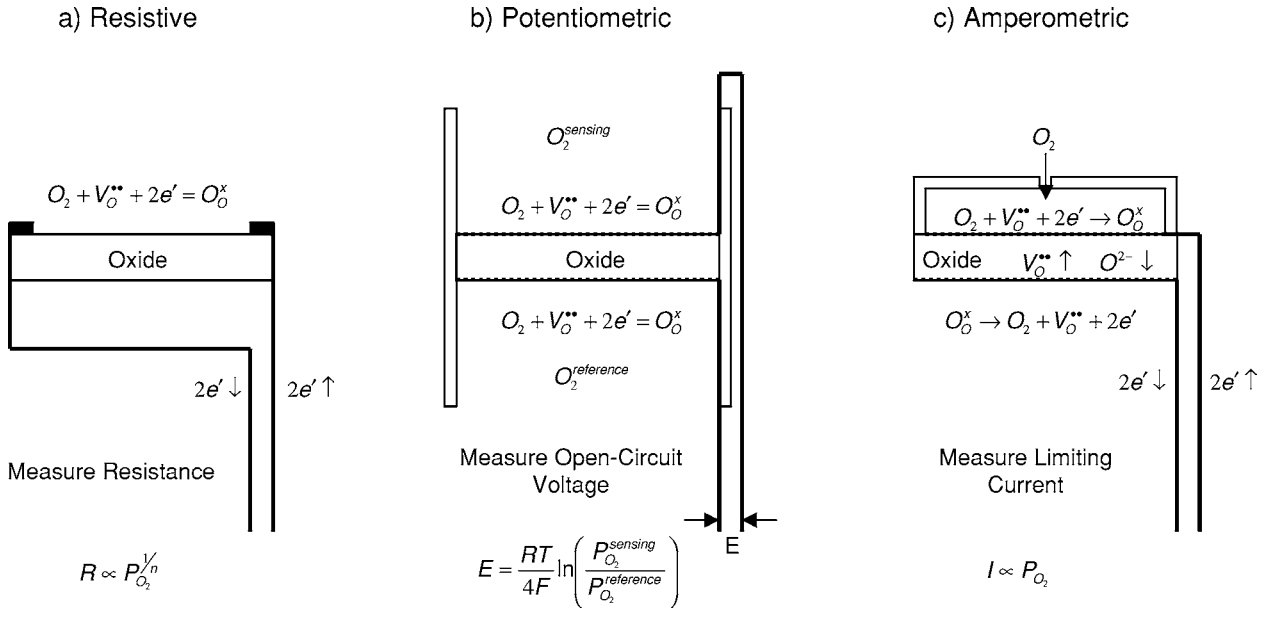

Figure 1 Schematic illustrations describing operation of (a) resistive-type, (b) potentiometric-type and (c) amperometric-type oxygen sensors.

Amperometric-type sensors (Fig. 1c) also use solid electrolytes, but in this case a voltage is applied across the electrolyte to pump oxygen from a small chamber into the surrounding atmosphere. The small chamber is connected to the sample gas with either a small orifice or a porous media, either of which limits gas diffusion. Initially, as the voltage applied across the electrolyte increases, the current increases as the amount of oxygen being pumped through the electrolyte increases. However, the rate of oxygen being pumped through the electrolyte eventually exceeds the rate at which oxygen can diffuse from the sample gas into the small chamber, so a limiting current is reached. The magnitude of this limiting current is proportional to the rate at which oxygen can diffuse through the small orifice or porous media, which is proportional to the oxygen partial pressure in the sample gas according to Fick's first law for steady-state diffusion. As compared to a potentiometric-type sensor, an amperometric-type sensor provides improved sensitivity in oxygen partial pressures near the reference oxygen partial pressure used in the potentiometric-type sensor. One example is in an internal combustion engines during lean-burn operation where the oxygen partial pressure in the exhaust gas (10^3 Pa) approaches that in air (2×10^4 Pa) [18].

3. Defects in oxides

The type of sensor in which a particular oxide is used depends on the types, concentrations and mobilities of the ionic and electronic defects. The defects prevalent in an oxide depend strongly on oxygen partial pressure, and this is commonly represented in Brouwer diagrams [21–23]. A schematic Brouwer diagram for an oxide, for which an anion Frenkel pair ($V_O^{\bullet\bullet} + O_i''$) is the intrinsic defect, and the concentrations of ionic defects are larger than those of electronic defects (i.e., electrons and holes), is shown in Fig. 2. At the stoichiometric composition, the concentration of oxygen vacancies and oxygen interstitials must be equal. At high oxygen partial pressures, excess oxygen can be incorporated through the formation of excess oxygen interstitials. Likewise at low oxygen partial pressures, a deficiency in oxygen content can be accommodated through the formation of excess oxygen vacancies. The concentrations of electronic defects are also dependent on oxygen partial pressure, as can be determined from the equilibrium constant for Reaction 1 (K_1).

$$K_1 = \frac{[O_O^x]}{P_{O_2}^{1/2} \cdot [V_O^{\bullet\bullet}] \cdot n^2} = \frac{1}{P_{O_2}^{1/2} \cdot [V_O^{\bullet\bullet}] \cdot n^2} \quad (2)$$

At low oxygen partial pressure, the concentrations of electrons (n) and oxygen vacancies are much larger than those of any other defects, so charge neutrality requires that,

$$2 \cdot [V_O^{\bullet\bullet}] = n \quad (3)$$

in which case, Equation 2 becomes.

$$K_1 = \frac{1}{P_{O_2}^{1/2} \cdot \left(\frac{n}{2}\right) \cdot n^2} \Rightarrow n = \left(\frac{2}{K_1}\right)^{1/3} \cdot P_{O_2}^{-1/6} \quad (4)$$

The concentrations of oxygen vacancies and electrons have the same oxygen partial pressure dependence and thus are represented by parallel lines in Fig. 2.

In intermediate oxygen partial pressures, where the concentration of intrinsic anion Frenkel pairs is high, the concentration of oxygen vacancies is much larger than the concentration of electrons, so Equation 2 becomes,

$$K_1 = \frac{1}{P_{O_2}^{1/2} \cdot [V_O^{\bullet\bullet}] \cdot n^2} \Rightarrow n = \left(\frac{1}{K_1 \cdot [V_O^{\bullet\bullet}]}\right)^{1/2} \cdot P_{O_2}^{-1/4} \quad (5)$$

where the concentration of oxygen vacancies is constant for a given temperature as determined by the energy of formation for an anion Frenkel pair. The relative magnitudes of the exponents in Equations 4 and 5 are

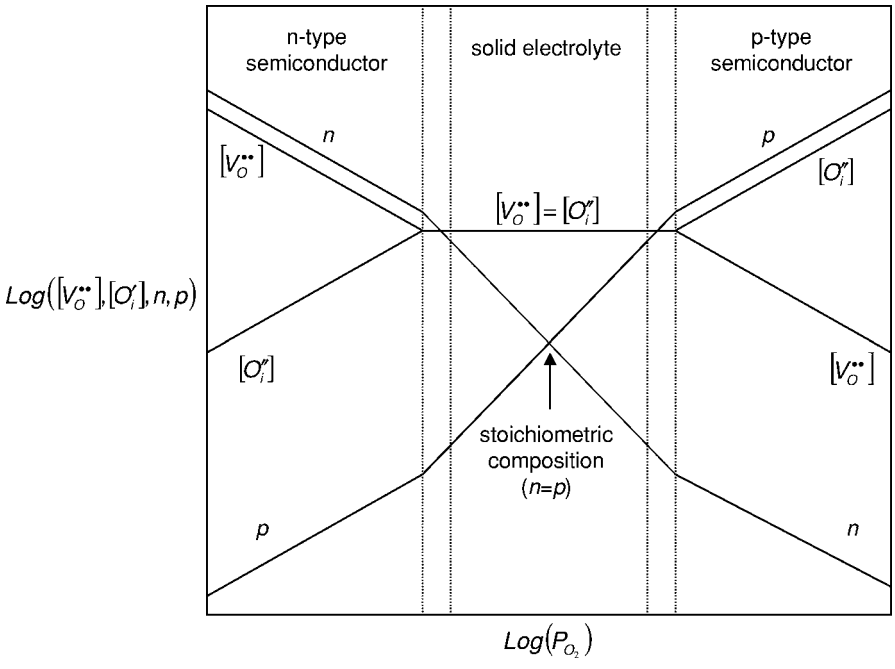

Figure 2 Schematic Brouwer diagram summarizing defects in oxide with anion Frenkel intrinsic defects.

reflected in the steeper slope for the electron concentration at intermediate oxygen partial pressures (slope = −1/4), as compared to that at low oxygen partial pressures (slope = −1/6). Similar equilibrium reactions can be used to determine the relationships among other defects. Likewise analogous diagrams can be constructed for systems with other predominant defects, such as materials with intrinsic Shottky pairs, or materials for which the concentration of electron-hole pairs is larger than that of the predominant intrinsic ionic defect [21]. Although the schematic diagram in Fig. 2 contains regions for three types of conduction, most oxides do not contain all regions.

The different regions in the Brouwer diagram are useful for different types of sensors. Resistive-type sensors rely on changes in conductivity (often particularly surface conductivity) due to changes in the defect concentrations through interaction with oxygen in the atmosphere [24, 25]. Thus, these sensors would be used in the regions labeled "*p*-type semiconductor" and "*n*-type semiconductor" in Fig. 2, where the defect concentration, and thus the conductivity, increases (*p*-type) or decreases (*n*-type) with increasing oxygen partial pressure.

Potentiometric- and amperometric-type sensors require that the ionic conductivity is much higher than the electronic conductivity, and thus would be used in intermediate oxygen partial pressures in the region labeled "solid electrolyte" in Fig. 2. Although some pure oxides are ionic conductors, often dopants are added to increase the concentration of ionic defects and extend the range over which the material is a solid electrolyte. For example, the most common solid oxide electrolyte, zirconia, is doped with other oxides. If zirconia is doped with yttria, yttrium ions will occupy zirconium sites and create oxygen vacancies according to the following reaction.

$$Y_2O_3 = 2Y'_{Zr} + 3O_O^x + V_O^{\bullet\bullet} \quad (6)$$

As the concentration of oxygen vacancies increases, the horizontal line representing the concentration of oxygen vacancies moves up, so the oxygen partial pressure at which this line intersects the line representing the electron concentration decreases, indicating that the onset of *n*-type semiconduction does not occur until a lower oxygen partial pressure. Similarly, *p*-type semiconduction will not occur until a higher oxygen partial pressure. Thus, in addition to increasing conductivity, doping can expand the range of oxygen partial pressures over which the oxide is a solid electrolyte. Doping can also affect the defect concentrations in the semiconducting regions, and thus can affect the performance of resistive-type sensors.

In the following sections, two prototypical sensor materials, titania and zirconia, will be discussed to illustrate how doping can affect the defect equilibria and transport properties on which oxygen sensors are based. Although the focus will be on oxygen sensors, some examples of uses of these materials in other types of sensors will be given.

4. Semiconducting oxide based sensors

One of the most commonly used materials in resistive-type oxygen sensors is titanium oxide (TiO_2), which has been used in sensors for measuring oxygen [26–33], carbon monoxide [7, 33–36], nitrous/nitric oxide [11, 34, 37], hydrocarbon gases [11, 36] and water vapor [36, 38]. Titania is most commonly used in the rutile crystal structure of TiO_2, but a reduced titanium oxide (Ti_3O_5) has been investigated for use in low oxygen partial pressures [39].

4.1. Defects in pure TiO_2

The defect structure of titania has been widely investigated and there are entire articles [40–44] and sections of articles [21, 45–49] which discuss the defect

structure of titania. Although there is some disagreement over the detailed defect structure, there is general agreement that titania is an oxygen-deficient oxide, and thus exhibits *n*-type conduction. The oxygen deficiency has been attributed to both oxygen vacancies and titanium interstitials. The most commonly proposed defect structure is that at intermediate oxygen partial pressures, oxygen vacancies are predominant, but that titanium interstitials become predominant at lower oxygen partial pressures. Some calculations of defect energies indicate that oxygen vacancies are favored [50, 51], but another suggests that titanium interstitials are slightly more stable [52], so defect models often contain mixed defects (oxygen vacancies and titanium interstitials) [53–55]. As the titania becomes more oxygen deficient and the defect concentration increases, the defects can form ordered structures or clusters [40, 47, 51, 55–57]. Calculations have indicated that planar extended defects are stable in titania [51, 57]. These defects grow into Crystallographic Shear Planes (CSP), which have been observed using Transmission Electron Microscopy (TEM) [58–61]. Further extension of these ordered defects results in the formation of separate phases, which are referred to as Magnéli phases [62–65] and have the general formula Ti_nO_{2n-1}.

Although the defect structure of titania is relatively complex, much of this complication is not critical to its use as a chemical sensor. For example, as apparent in Equations 4 and 5, the oxygen partial pressure dependence for conductivity (σ), or resisitivity (ρ), of a semiconducting oxide is in the form,

$$\sigma = \frac{1}{\rho} \propto P_{O_2}^{1/m} \tag{7}$$

Note that "*n*" is frequently used in the literature as the exponent, but "*m*" is used here to avoid confusion with the electron concentration. The value of *m* for titania can vary from −4 to −6, and often is not an integer, which indicates that there is more than one predominant defect. However, as long as the oxygen partial pressure dependence is repeatable and stable over time, the material can be used in a sensor, even if the specific defect chemistry is not completely understood.

4.2. Electron acceptor doped TiO_2

One electron-acceptor dopant which is commonly added to titania is chromia. The following charge balance reaction,

$$[Cr'_{Ti}] + n = 4 \cdot \lfloor Ti_i^{\bullet\bullet\bullet\bullet} \rfloor + p \tag{8}$$

has been proposed to describe the effect of chromia additions on the defect concentrations in titania. Fig. 3 shows that, as predicted by Equation 8, chromia additions decrease the *n*-type electronic conductivity of titania [66, 67]. Carpentier *et al.* [66] also determined the ionic conductivity from impedance spectroscopy and found that the ionic conductivity increased with increasing chromia content. The oxygen partial pressure dependence for pure titania in Fig. 3 ($m = -5$) suggests that the predominant ionic defect is a titanium interstitial, the conductivity of which can be increased by the following reaction.

$$Ti_{Ti}^{x} + 2O_O^x + 2Cr_2O_3 = 4Cr'_{Ti} + Ti_i^{\bullet\bullet\bullet\bullet} + 8O_O^x \tag{9}$$

The increase in the magnitude of the oxygen partial pressure dependence (i.e., decrease in value of *m*) with chromia additions is attributed to the ionic point defect concentration being determined by the dopant level, rather than by the equilibrium with the oxygen in the atmosphere [66, 67]. Another result of chromia additions, also expected from Equation 8, is the onset of *p*-type conductivity at high oxygen partial pressures. This effect is shown more clearly in Fig. 4, which also includes results for alumina additions [68]. The

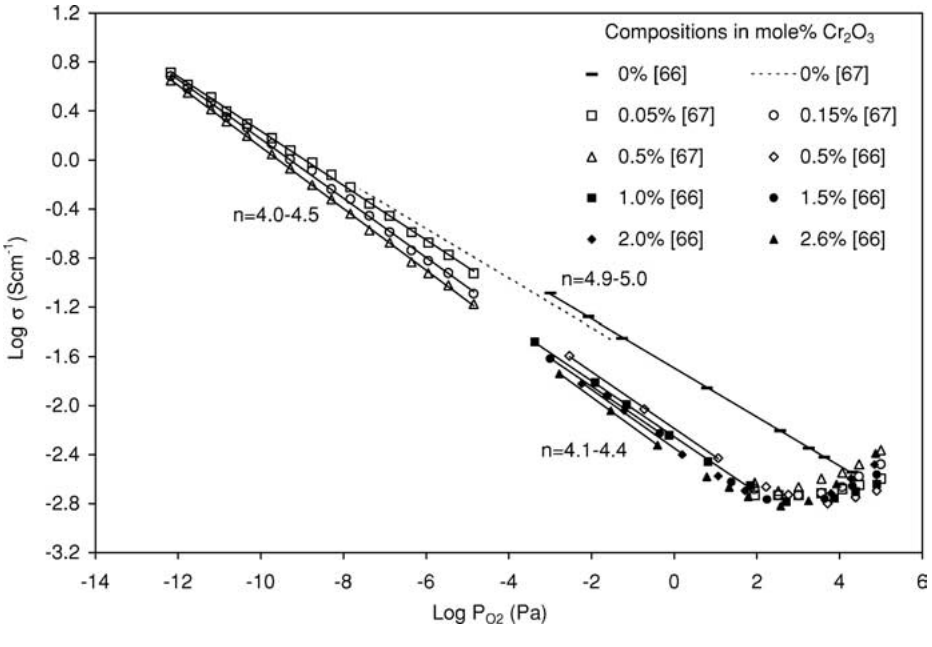

Figure 3 Conductivity of Cr_2O_3-doped TiO_2 at 1273 K [66, 67].

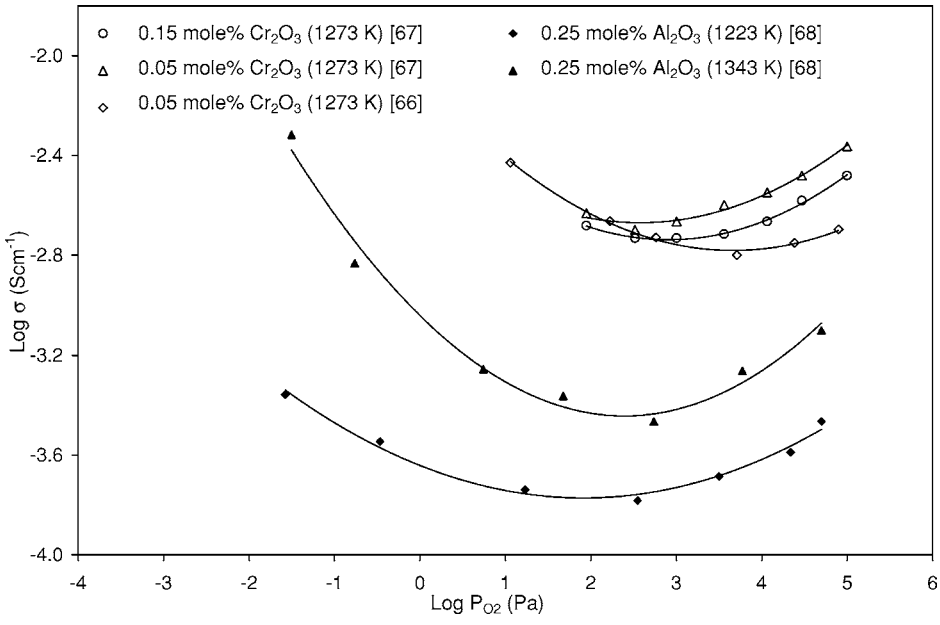

Figure 4 Conductivity of Cr_2O_3- and Al_2O_3-doped TiO_2 at 1223–1343 K [66–68].

minimum in the conductivity indicates the transition from *n*-type to *p*-type conduction. Yahia [68] also measured the thermoelectric effect and observed a change in sign of the Seebeck coefficient in the same oxygen partial pressure range. Bernasek *et al.* [69] also observed a transition from *p*-type to *n*-type conduction in chromia-doped titania and found that the transition depended on the chromia level. The effects of dopants on the conductivity are so significant that even impurity level concentrations of dopants, especially aluminum and iron, have caused problems in device performance [70].

Chromium has been observed to interact with other defects, such as CSP, in titania [71–76]. Up to 7.5% chromium (3.75% Cr_2O_3) can dissolve in the rutile phase $(Ti,Cr)O_{2-x}$ and will be present in the form of point defects. While the specific nature of the chromium defect is not completely understood, it appears that chromium may occupy either interstitial or substitutional sites. Substitutional chromium results in the formation of additional oxygen vacancies for charge compensation. With higher chromium contents, these point defects associate to form defect complexes eventually leading to the formation of CSP defects and Magnéli-type phases with the general formula $Cr_2Ti_{n-2}O_{2n-1}$.

4.3. Electron donor doped TiO_2

The conductivities of titania doped with niobium oxide (Nb_2O_5), which acts as an electron donor, are shown in Fig. 5 [54, 77]. With sufficient doping, there is an oxygen partial pressure independent region, which has

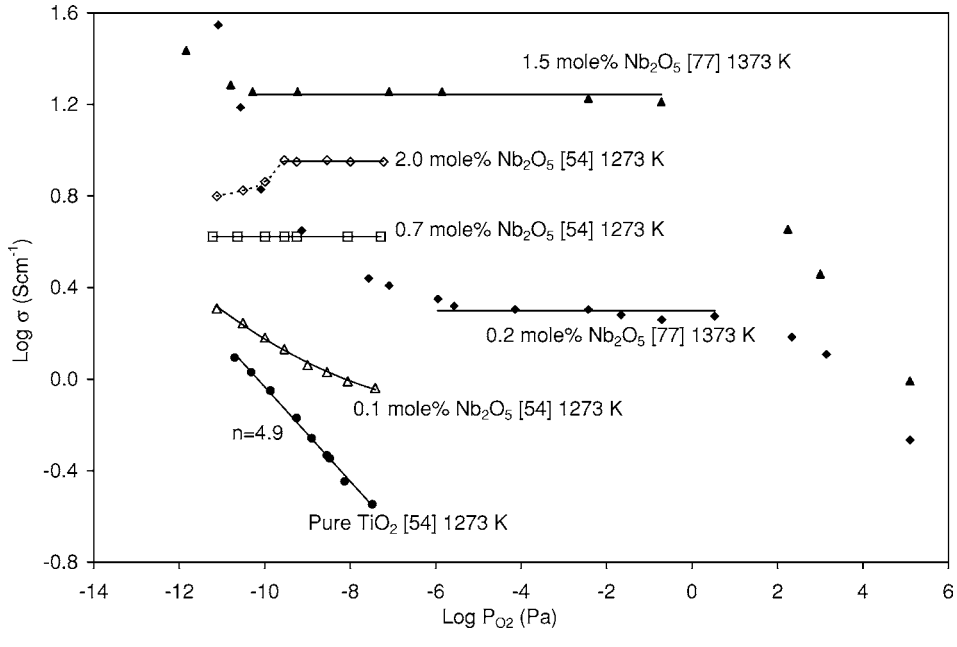

Figure 5 Conductivity of Nb_2O_5-doped TiO_2 at 1273–1373 K [54, 77].

been attributed to the electron concentration being fixed by the dopant level according to the following reaction.

$$Nb_2O_5 = 2Nb_{Ti}^{\cdot} + 4O_O^x + 2e' + \frac{1}{2}O_2 \qquad (10)$$

Reflectance and Electron Spin Resonance (ESR) measurements on niobia-doped titania also suggest that niobium acts as an electron donor [78]. At higher oxygen partial pressures the decrease in negative slope is attributed to the niobium (Nb^{5+}) defect being compensated for with an ionic defect (titanium vacancy or oxygen interstitial), with a resulting increase in electron concentration. Overall, niobia doping increases the conductivity, but decreases the range over which titania has sufficiently high oxygen partial pressure dependent conductivity for use in a resistive-type oxygen sensor.

Niobium can interact with other defects in titania. For example, X-ray diffraction measurements have shown that niobium increases the solubility of aluminum [79], which, as discussed above, acts as a *p*-type dopant in titania. Calculations indicating that the enthalpy of the niobium substitutional defect is lower in the presence of aluminum provide additional evidence for defect interaction [80]. Work function measurements have also suggested interaction of niobium with trivalent metal impurities, some of which (e.g., aluminum) tend to segregate to the surface [69]. Possible surface segregation is particularly important in resistive-type sensors, which often rely disproportionately on surface conduction, so interference from impurities may be enhanced if the interfering elements are concentrated near the surface.

4.4. Effect of dopants on sensor response

As shown above, chromia is added to titania to create a *p*-type semiconductor. Chromia-doped titania based sensors have improved sensitivity [26, 29] and faster response [26, 28, 29, 69] as compared to undoped titania. Niobia additions, on the other hand, can improve the sensitivity [31], but often result in a slower response [28, 69]. However, the sensor performance depends on the specific conditions. For example, Sharma *et al.* [29] reported that chromia additions provide the faster response at 973 K, but niobia additions provide the faster response at 823 K. In addition to sensitivity and response time, linearity of the response is important to simplify signal processing. For example, Zakrzewski *et al.* [28] determined that niobia additions increase the response time, but also provide a more monotonic, and thus more easily interpreted, output. Additions can also affect the morphology of the materials. For example, the addition of molybdenum oxide (MoO_3) to titania results in a film with lower resistivity and higher porosity, both of which can improve response time [27].

Resistance-based sensors using titania are also used for sensing gases other than oxygen. Such sensors typically rely on the effect of the equilibrium between the gas of interest and the oxide surface to cause a change in the defect concentration, and thus conductivity, at the surface. The sensitivity to other gases requires establishing the appropriate surface reaction, which is often accomplished through doping of the oxide. For example, niobium has been shown to enhance sensitivity to NO_2 [37] and CO [35], while yttrium enhances sensitivity to CO [7] and NO [11]. Other examples include alumina and zirconia which have been shown to enhance sensitivity to hydrogen [7] and methane [11], respectively. Sometimes, sensitivity to a particular gas is accomplished by reducing sensitivity to an interfering species. For example, tin has been shown to reduce sensitivity to CO and methane [36], while aluminum has been used to improve a NO_2 sensor by reducing interference from oxygen. A combination of sensor compositions, which have different responses to different gases, can thus be used to create a sensor array to characterize a multi-component gas mixture [33].

A common addition to titania-based sensor for use in detecting reducing gases, such as CO [81, 82] and H_2 [82], is tin. Tin oxide (SnO_2) also forms the rutile crystal structure and forms a solid solution with titania. Thus, just as tin oxide can be used as a dopant in titania, titania has been used as a dopant in tin oxide [83–85]. Some other oxides material used for resistance-type sensors include perovskite-based oxides [86–89] and ceria-based oxides [90–92].

5. Solid electrolyte based sensors

Solid electrolyte based sensors include both potentiometric-type and amperometric-type sensors. Although there are differences in the relative importance of certain properties, many of the issues are the same, so materials for both types of solid electrolyte-based sensors will be discussed in the same section.

5.1. Solid oxide electrolytes

In 1957, Kuikkola and Wagner [93] demonstrated that solid electrolytes could be used to measure oxygen partial pressures established by metal/metal-oxide mixtures, and this concept was subsequently used in the development of solid electrolyte based oxygen sensors. There are several types of chemical sensors based on solid electrolytes [94–97]. Weppner [94] has classified potentiometric solid electrolyte based sensors according to the equilibrium required to relate chemical activity of the species to be measured to that which is mobile in the electrolyte. Oxygen sensors using oxide-ion conducting electrolytes do not require additional equilibria, which is a Type I sensor according to Weppner's classification. Considerations in the selection of a solid electrolyte from the numerous candidate oxide electrolytes [98, 99] include conductivity, chemical stability, as well as issues such as cost, availability and mechanical strength. In light of the previous discussion, one important consideration is the onset of electronic conduction, which can lead to erroneous results both in potentiometric-type [100, 101] and amperometric-type [102] sensors.

The most common solid oxide electrolyte is zirconia, which forms the cubic fluorite structure. The cubic fluorite structure is named after the mineral calcium fluoride (CaF_2), for which the intrinsic ionic defect is an

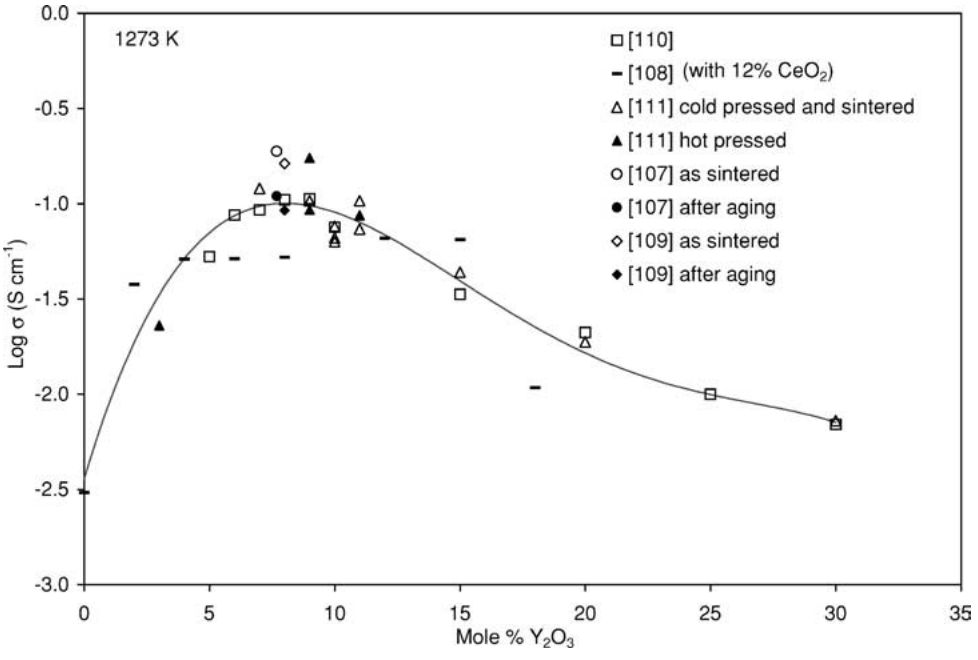

Figure 6 Conductivity of Y_2O_3-doped ZrO_2 at 1273 K [107–111].

anion Frenkel defect. Zirconia is generally considered to also form anion Frenkel defects [22] and there are calculations that indicate this is the lowest energy defect [103]. However, there have been reports of calculations which suggest that the energy of a Shottky-type defect in zirconia is lower than that of a Frenkel-type defect [104]. In addition, some elastic constant measurements suggest that the defect structure of zirconia is different from that of calcium fluoride [105]. However, zirconia is generally doped such that the concentration of oxygen vacancies is much larger than that of the compensating intrinsic ionic defect (oxygen interstitial or zirconium vacancies), so the important ionic defect in zirconia based electrolytes is the oxygen vacancy [106].

5.2. Conductivity of zirconia

Pure zirconia forms the cubic fluorite structure only at high temperatures, so other oxides must be added to stabilize the cubic fluorite structure at low temperatures. One of the most common stabilizers is yttria, which, as shown above in Equation 6, has the added benefit of increasing the concentration of oxygen vacancies. Fig. 6 shows the effect of yttria-additions on the conductivity of Yttria Stabilized Zirconia (YSZ) [107–111]. Although not fundamentally important to the sensor operation, insufficiently low conductivity can lead to a slow response time, particularly at low temperatures. As expected, with an increase in the concentration of charge carriers from the addition of yttria, the conductivity increases. However, beyond about 9 mol% Y_2O_3, the conductivity decreases. This decrease is generally attributed to association among defects [112]. This is supported by calculations indicating that the activation energy for oxygen vacancy motion near a dopant is higher than that away from the dopant [113]. In addition, neutron diffraction [114], X-ray diffraction [115–120] and energy calculations [121–124] indicate that the distribution of oxygen vacancies in zirconia is not completely random. These results generally indicate that oxygen vacancies prefer to be located near smaller cations, which in the case of YSZ would be the zirconium ions. Such a tendency towards ordering limits freedom of motion and thus tends to decrease mobility.

Fig. 7 shows the results of calculations of defect energies [104, 125, 126] for some ions which have been used as dopants in zirconia. The ionic radii used are those for eight-fold coordination as reported by Shannon [127]. Results are given for both nearest neighbor (*nn*) and next nearest neighbor (*nnn*) configurations, which are shown in Fig. 8. There are more extended defect complexes, which have lower energies [104, 125, 128], but the simple associations are used here to discuss trends in doping. In most cases the *nnn* configuration has the lowest energy, and, at least for trivalent ions, defect association becomes more favorable as the size of the dopant cation increases. The other notable trend is that the energies for divalent dopants (Mg^{2+} and Ca^{2+}) are lower than those for trivalent ions. Increased defect association will lead to decreased mobility and thus decreased conductivity.

Fig. 9 summarizes some results for the conductivity of calcia-stabilized zirconia [101, 110, 111, 129]. The line is the trendline from Fig. 6, which is included to allow for comparison with YSZ. Consistent with the more stable defect association indicated in Fig. 7, the conductivity of calcia-stabilized zirconia is lower than that of YSZ. In addition, internal friction measurements indicate that oxygen vacancies are more strongly bonded in calcia-stabilized zirconia than in YSZ [130].

Dopant ions that are of similar size as the host ion tend to have lower association energies, and thus higher mobility, so doping with a smaller ion (as compared to Y^{3+} or Ca^{2+}), such as Sc^{3+}, should result in a higher conductivity [121]. Fig. 10 shows that the conductivity of scandia-stabilized zirconia is, in general, higher than that of YSZ [109, 111, 131]. There have, however, been reports of degradation of conductivity with

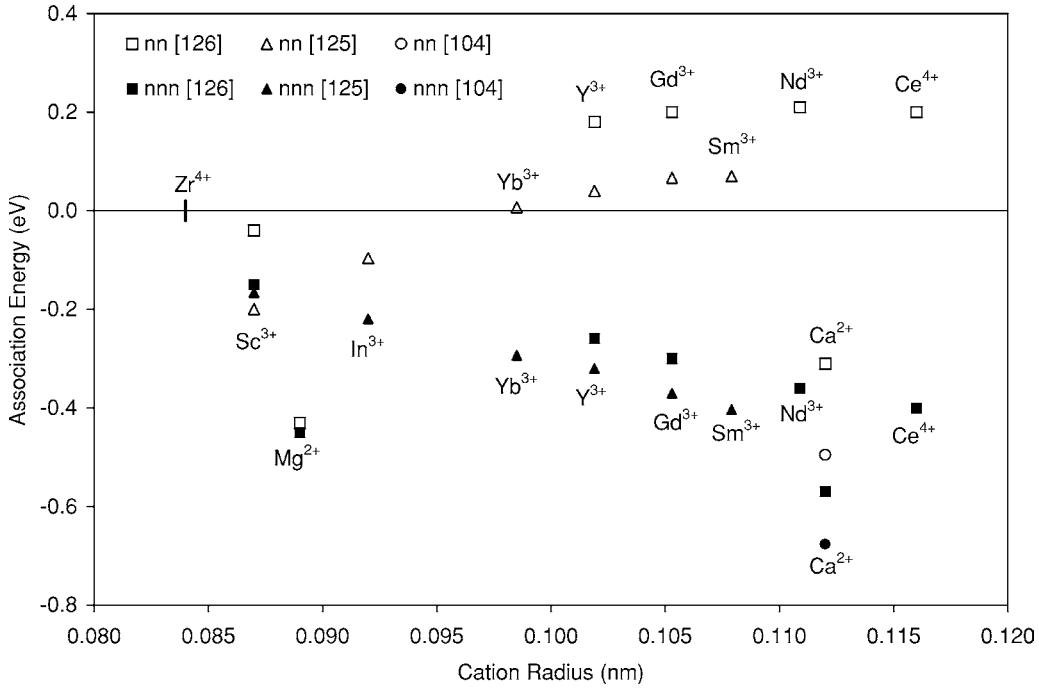

Figure 7 Calculated energy of nearest neighbor (*nn*) and next nearest neighbor (*nnn*) dopant—oxygen pair vacancy associations in doped zirconia [104, 125, 126].

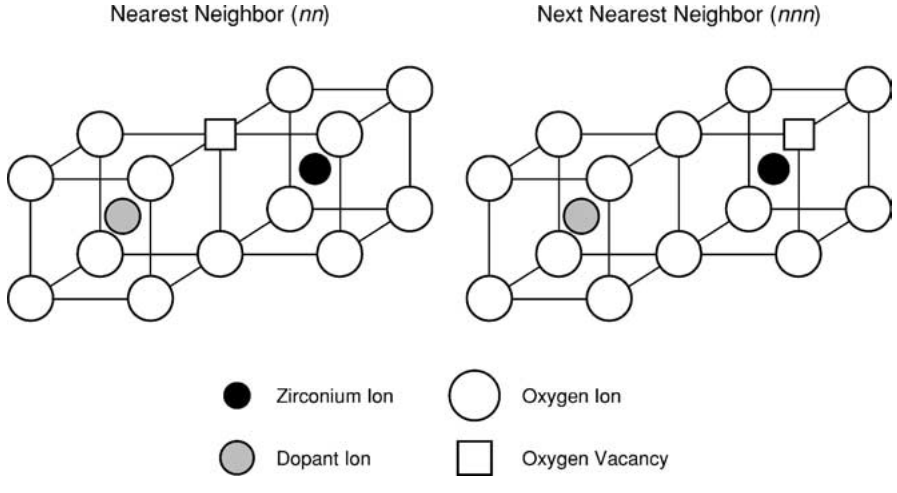

Figure 8 Schematics of nearest neighbor (*nn*) and next nearest neighbor (*nnn*) dopant—oxygen pair vacancy associations.

aging of scandia-stabilized zirconia. For example, the decrease in conductivity during aging of zirconia containing 8 mol% Sc_2O_3 has been shown to be much larger than that for zirconia containing 8 mol% Y_2O_3 [109]. However, with larger scandia additions (11 mol% Sc_2O_3) the decrease in conductivity during aging is minimal [109, 131].

The conductivities of some zirconia-based materials at lower temperatures are shown in Fig. 11 [132–136]. The niobia- and alumina-doped materials also contain 8–9% Y_2O_3, and are thus fully stabilized into the cubic fluorite structure. The materials containing india or yttria, however, do not contain sufficient stabilizer and are thus in the tetragonal crystal structure. Calculations have shown that defect pairs are more stable in the tetragonal structure as compared to the cubic structure [112], which may explain the decrease in conductivity with increasing india additions even for relatively small india additions. For india-doping, the maximum conductivity is in the cubic phase at the composition of the tetragonal—cubic phase boundary [137]. India additions to YSZ have also been shown to improve the resistance to aging [107].

Dopant additions can also have indirect benefits to the performance of the electrolyte materials. For example, alumina additions have been shown to enhance the sintering of zirconia [138, 139], which can lead to improved quality and/or reduced sintering times or temperatures.

5.3. Other solid electrolyte based sensor

Although zirconia based sensors are the most common solid electrolyte based sensors, other oxide electrolytes, some of which also form the cubic fluorite structure, are being used or being developed for oxygen sensors [98, 99, 140]. Examples of alternative oxide electrolytes include bismuth oxide and oxides with the pyrochlore

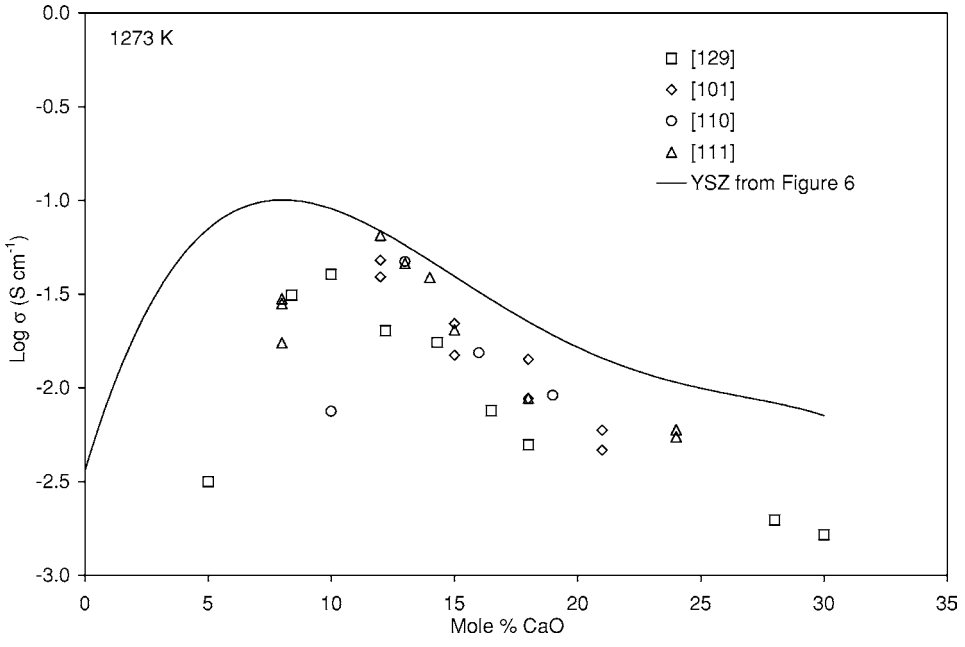

Figure 9 Conductivity of CaO-doped ZrO_2 at 1273 K [101, 110, 111, 129].

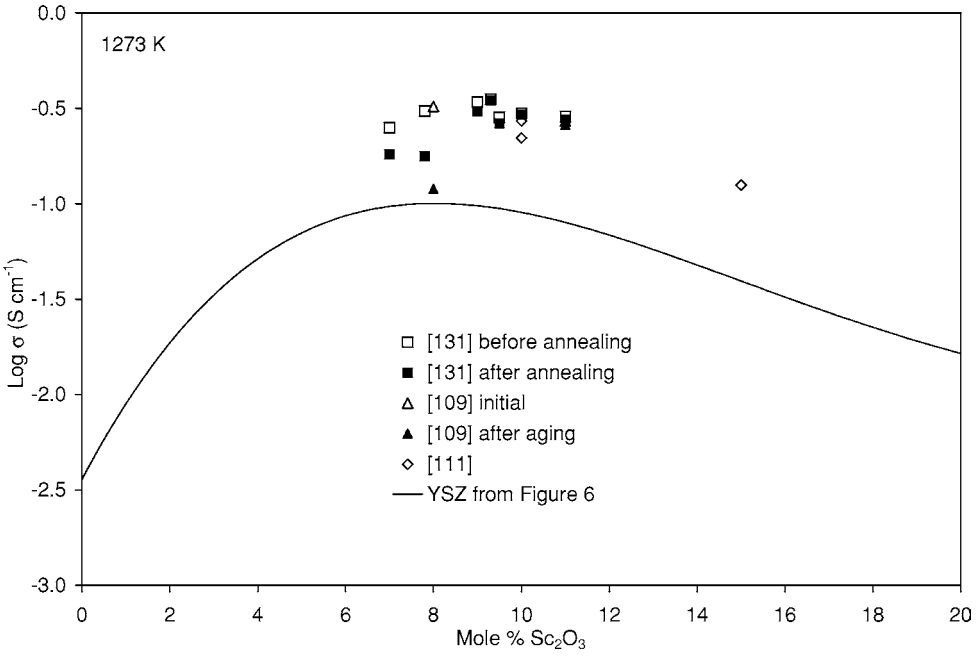

Figure 10 Conductivity of Sc_2O_3-doped ZrO_2 at 1273 K [109, 111, 131].

structure. In addition, Type II or Type III sensors [94] can also be used for sensing oxygen. Type II sensors use electrolytes which contain the species being measured, but that species is not mobile in the electrolyte. For an oxygen sensor, this would be an oxygen-containing material which conducts an ion other than oxygen. An example of this is the use of phosphate-based proton-conducting electrolytes for oxygen sensors [141, 142]. Type III sensors use an electrolyte that does not contain the species to be measured, but contains a phase, referred to as an auxiliary electrode, which equilibrates with the species to be measured to establish a chemical potential to which the electrolyte will respond. Many fluoride compounds are excellent solid electrolytes, and have been used as Type III oxygen sensors [143]. These sensors rely on the addition, or *in situ* formation, of an oxide phase, which equilibrates with oxygen in the environment and the fluoride electrolyte to establish a measurable fluorine activity. Auxiliary electrodes can also be applied to zirconia to measure gases other than oxygen. For example, the addition of the appropriate carbonate or nitrate phase to zirconia-based sensors provides the response required for measuring CO [144], CO_2 [145] or NO_2 [144, 146].

Although zirconia is generally used as a solid electrolyte, it can be doped to produce a mixed conductor [147–151]. While this can provide the oxygen partial pressure dependent conductivity needed for a resistive-type oxygen sensor [147], the more common objective is a mixed conducting electrode for a solid oxide fuel cell [148–151]. Such an electrode eliminates the need for three-phase contact and thus increases the effective

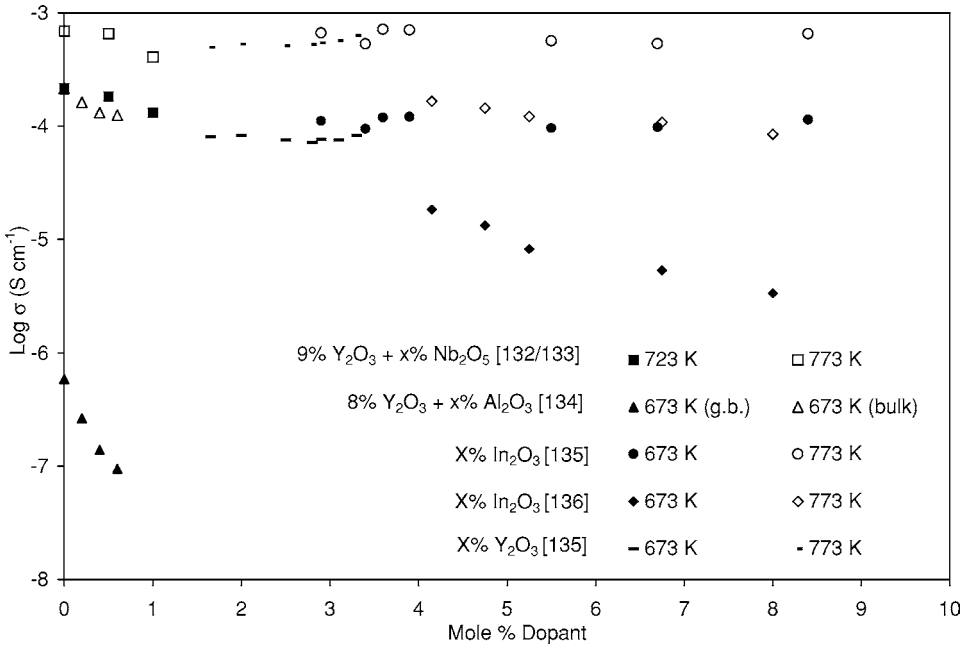

Figure 11 Conductivity of Y_2O_3-, Nb_2O_5-, Al_2O_3-, and In_2O_3-doped ZrO_2 at 673–773 K [132–136].

area of the electrode. Interestingly, in light of the focus of this paper, one of the dopants used for this purpose is titania, which has been added to produce a mixed-conducting zirconia-based material [149–151].

6. Conclusions

Point defects and their interactions are important in all the common approaches to the development of oxygen sensors for improving the efficiency of combustion processes. Demonstrated success of current sensors will lead to new applications, which may require improved materials and modified approaches. Some possible areas for improvement include expanded operating range (temperature and/or oxygen partial pressure), improved chemical stability and faster response time. Improved understanding of the defect chemistry will help to address these requirements and guide the development of new sensors for future applications.

References

1. G. MÜLLER, G. KRÖTZ and J. SCHALK, *Phys. Stat. Sol.* (a) **185**(1) (2001) 1.
2. W. J. FLEMMING, *IEEE Sensors J.* **1**(4) (2001) 296.
3. J. RIEGEL, H. NEUMANN and H.-M. WIEDENMANN, *Sol. St. Ionics* **152–153** (2002) 783.
4. J. ZOSEL, F. DE BLAUWE and U. GUTH, *Adv. Eng. Mater.* **3**(10) (2001) 797.
5. E. L. BROSHA, R. MUKUNDAN, D. R. BROWN, F. H. GARZON and J. H. VISSER, *Sol. St. Ionics* **148** (2002) 61.
6. R. MUKUNDAN, E. L. BROSHA and F. H. GARZON, in "Ceramic Transactions (Chemical Sensors for Hostile Environments)," Vol. 130, edited by G. M. Kale, S. A. Akbar and M. Liu (The American Ceramic Society, Westerville, OH, 2002) p. 1.
7. A. M. AZAD, L. B. YOUNKMAN, S. A. AKBAR, S. AHMED and G. RIZZONI, in "Ceramic Transactions (Role of Ceramics in Advanced Electrochemical Systems)," Vol. 65, edited by P. N. Kumta, G. S. Rohrer and U. Balachandran (The American Ceramic Society, Westerville, OH, 1996) p. 343.
8. N. GUILLET, R. LALAUZE, J.-P. VIRICELLE, C. PIJOLAT and L. MONTANARO, *Mater. Sci. Eng.* C **21** (2002) 97.
9. C. PIJOLAT, C. PUPIER, M. SAUVAN, G. TOURNIER and R. LALAUZE, *Sensors and Actuators* B **59** (1999) 195.
10. T. SCHULTE, R. WASER, E. W. J. RÖMER, H. J. M. BOUWMEESTER, U. NIGGE and H.-D. WIEMHÖFER, *J. Eur. Ceram. Soc.* **21** (2001) 1971.
11. S. A. AKBAR, C. C. WANG, L. WANG and D. J. COLLINS, in "Ceramic Transactions (Role of Ceramics in Advanced Electrochemical Systems)," Vol. 65, edited by P. N. Kumta, G. S. Rohrer and U. Balachandran (The American Ceramic Society, Westerville, OH, 1996) p. 331.
12. I. SIMON and M. ARNDT, *Sensors and Actuators* A **97/98** (2002) 104.
13. A. D. BRAILSFORD, M. YUSSOUFF, E. M. LOGOTHETIS, T. WANG and R. E. SOLTIS, *ibid.* B **42** (1997) 15.
14. A. D. BRAILSFORD, M. YUSSOUFF and E. M. LOGOTHETIS, *ibid.* **44** (1997) 321.
15. N. DOCQUIER and S. CANDEL, *Prog. Energy Combustion Sci.* **28** (2002) 107.
16. H. KUBLER, *Wood and Fiber Sci.* **24**(2) (1992) 141.
17. T. TAKEUCHI, *Sensors and Actuators* B **14** (1988) 109.
18. A. M. AZAD, S. A. AKBAR, S. G. MHAISALKAR, L. D. BIRKEFELD and K. S. GOTO, *J. Electrochem. Soc.* **139**(12) (1992) 3690.
19. J. R. STETTER, W. R. PENROSE and S. YAO, *ibid.* **150**(2) (2003) S11.
20. N. YAMAZOE and N. MIURA, *Sensors and Actuators* B **20** (1994) 95.
21. P. KOFSTAD, "Nonstoichiometry, Diffusion, and Electrical Conductivity in Binary Metal Oxides," edited by Robert E. Krieger (Publishing Co., Malabar, FL, 1983).
22. J. SCHOONMAN, in "CRC Handbook of Solid State Electrochemistry," edited by P. J. Gellings and H. J. M. Bouwmeester (CRC Press, Boca Raton, FL, 1997) p. 161.
23. R. A. HUGGINS, *Sol. St. Ionics* **143** (2001) 3.
24. C. C. WANG, S. A. AKBAR and M. J. MADOU, *J. Electroceram.* **2**(4) (1998) 273.
25. V. LANTTO, T. T. RANTALA and T. S. RANTALA, *J. Eur. Ceram. Soc.* **21** (2001) 1961.
26. R. K. SHARMA, M. C. BHATNAGAR and G. L. SHARMA, *Sensors and Actuators* B **45** (1997) 209.
27. Y. LI, K. GALATSIS, W. WLODARSKI, M. GHANTASALA, S. RUSSO, J. GORMAN, S.

SANTUCCI and M. PASSACANTANDO, *J. Vac. Sci. Tech.* A **19**(3) (2001) 904.
28. K. ZAKRZEWSKA, M. RADECKA and M. RĘKAS, *Thin Solid Films* **310** (1997) 161.
29. R. K. SHARMA and M. C. BHATNAGAR, *Sensors and Actuators* B **56** (1999) 215.
30. S. HASEGAWA, Y. SASAKI and S. MATSUHARA, *ibid.* **13/14** (1993) 509.
31. M. Z. ATASHBAR, H. T. SUN, B. GONG, W. WLODARSKI and R. LAMB, *Thin Solid Films* **326** (1998) 238.
32. N. NICOLOSO, *Ber. Bunsen-Ger. Phys. Chem.* **94** (1990) 731.
33. M. L. FRANK, M. D. FULKERSON, B. R. PATTON and P. K. DUTTA, *Sensors and Actuators* B **87** (2002) 471.
34. J. HUUSKO, V. LANTTO and H. TORVELA, *ibid.* **15/16** (1993) 245.
35. G. S. HENSHAW, L. MORRIS, L. J. GELLMAN and D. E. WILLIAMS, *J. Mater. Chem.* **6**(12) (1996) 1883.
36. V. DUSASTRE and D. E. WILLIAMS, *ibid.* **9** (1999) 445.
37. Y. LI, W. WLODARSKI, K. GALATSIS, S. H. MOSLIH, J. COLE, S. RUSSO and N. ROCKELMANN, *Sensors and Actuators* B **83** (2002) 160.
38. R. ZANONI, G. RIGHINI, A. MONTENERO, G. GNAPPI, G. MONTESPERELLI, E. TRAVERSA and G. GUSMANO, *Surf. Int. Anal.* **22** (1994) 376.
39. L. ZHENG, *Sensors and Actuators* B **88** (2003) 115.
40. T. HURLEN, *Acta Chem. Scand.* **13**(2) (1959) 365.
41. A. VON HIPPEL, J. KALNAJS and W. B. WESTPHAL, *J. Phys. Chem. Solids* **23** (1962) 779.
42. F. A. GRANT, *Rev. Mod. Phys.* **31**(3) (1959) 646.
43. F. MILLOT, M.-G. BLANCHIN, R. TÉTOT, J.-F. MARUCCO, B. POUMELLEC, C. PICARD and B. TOUZELIN, *Prog. Sol. St. Chem.* **17** (1985) 263.
44. H. P. R. FREDERIKSE, *J. Appl. Phys.* **32**(10 Suppl) (1961) 2211.
45. A. ATKINSON, in "Adv. Ceram.: Nonstoichiometric Compounds," Vol. 23, edited by C. R. A. Catlow and W. C. Mackrodt (The American Ceramic Soc., Westerville, OH, 1987) p. 3.
46. H. O. FINKLEA, in "Semiconductor Electrodes," edited by H. O. Finklea (Elsevier, Amsterdam, 1988) p. 43.
47. J. B. GOODENOUGH, *Prog. Solid State Chem.* **5** (1971) 149.
48. H. J. MATZKE, in "Nonstoichiometric Oxides," edited by O. Toft Sørensen (Academic Press, New York, NY, 1981) p. 155.
49. D. M. SMYTH, *Prog. Sol. St. Chem.* **15** (1984) 145.
50. C. R. A. CATLOW, R. JAMES and M. J. NORGETT, *J. Phys. (Paris) Colloq.* **C7** (1976) 443.
51. C. R. A. CATLOW and R. JAMES, *Proc. Royal Soc. London* A **384** (1982) 157.
52. H. SAWATARI, E. IGUCHI and R. J. D. TILLEY, *J. Phys. Chem. Solids* **43**(12) (1982) 1147.
53. M. AONO and R. R. HASIGUTI, *Phys. Rev.* B **48**(17) (1993) 12406.
54. G. LEVIN and C. J. ROSA, *Z. Metallkde.* **70**(10) (1979) 646.
55. N. YU and J. W. HALLEY, *Phys. Rev.* B **51**(8) (1995) 4768.
56. C. MEIS and J. L. FLECHE, *Sol. St. Ionics* **101–103** (1997) 333.
57. A. N. CORMACK, C. M. FREEMAN, C. R. A. CATLOW and R. L. ROYLE, in "Adv. Ceram.: Nonstoichiometric Compounds," Vol. 23 edited by C. R. A. Catlow and W. C. Mackrodt (The American Ceramic Soc., Westerville, OH, 1987) p. 283.
58. L. A. BURSILL and B. G. HYDE, *Prog. Sol. St. Chem.* **7** (1972) 177.
59. R. J. D. TILLEY, in "Defect Crystal Chemistry and Its Applications" (Blackie & Son, Glasgow, 1987) p. 194.
60. M. G. BLANCHIN and L. A. BURSILL, *Phys. Stat. Sol.* (a) **86** (1984) 101.
61. M. G. BLANCHIN, P. FAISANT, C. PICARD, M. EZZO and G. FONTAINE, *ibid.* **60** (1980) 357.
62. S. ANDERSSON, B. COLLÉN, G. KRUUSE, U. KUYLENSTIERNA, A. MAGNÉLI, H. PESTMALIS and S. ÅSBRINK, *Acta Chem. Scand.* **11**(10) (1957) 1653.
63. S. ANDERSSON, B. COLLÉN, U. KUYLENSTIERNA and A. MAGNÉLI, *ibid.* **11**(10) (1957) 1641.
64. B.-O. MARINDER, E. DORM and M. SELEBORG, *ibid.* **16**(2) (1962) 293.
65. S. ANDERSSON and A. MAGNÉLI, *Naturwissenschaften* **42** (1956) 495.
66. J.-L. CARPENTIER, A. LEBRUN and F. PERDU, *J. Phys. Chem. Sol.* **50**(2) (1989) 145.
67. E. TANI and J. F. BAUMARD, *J. Sol. St. Chem.* **32** (1980) 105.
68. J. YAHIA, *Phys. Rev.* **130**(5) (1963) 1711.
69. A. BERNASIK, M. RADECKA, M. RĘKAS and M. SLOMA, *Appl. Surf. Sci.* **65/66** (1993) 240.
70. M. F. YAN and W. W. RHODES, *J. Appl. Phys.* **53**(12) (1982) 8809.
71. L. A. BURSILL and M. G. BLANCHIN, *J. Phys. Lett.* **44** (1983) 165.
72. L. A. BURSILL and S. G. JUN, *J. Sol. St. Chem.* **51** (1984) 388.
73. L. A. BURSILL, M. G. BLANCHIN and D. J. SMITH, *Phil. Mag.* A **50**(4) (1984) 453.
74. L. A. BURSILL, D. J. SMITH and P. J. LIN, *J. Sol. St. Chem.* **56** (1985) 203.
75. D. K. PHILP and L. A. BURSILL, *ibid.* **10** (1974) 357.
76. R. M. GIBB and J. S. ANDERSON, *ibid.* **4** (1972) 379.
77. M.-H. KIM, S.-I. LEE, T.-K. SONG, H. PARK, W. CHOI, H.-I. YOO and T.-G. PARK, *Korean J. Chem. Eng.* **18**(6) (2001) 873.
78. M. VALIGI, D. CORDISCHI, G. MINELLI, P. NATALE, P. PORTA and C. P. KEIJZERS, *J. Sol. St. Chem.* **77** (1988) 255.
79. R. A. SLEPETYS and P. A. VAUGHAN, *J. Phys. Chem.* **73**(7) (1969) 2157.
80. D. C. SAYLE, C. R. A. CATLOW, M.-A. PERRIN and P. NORTIER, *J. Phys. Chem. Solids* **56**(6) (1995) 799.
81. O. RENAULT, A. V. TADEEV, G. DELABOUGLISE and M. LABEAU, *Sensors and Actuators* B **59** (1999) 260.
82. Z. A. ANSARI, S. G. ANSARI, T. KO and J.-H. OH, *ibid.* **87** (2002) 105.
83. W.-Y. CHUNG, D.-D. LEE and B.-K. SOHN, *Thin Solid Films* **221** (1992) 304.
84. N. RADECKA, K. ZAKRZEWSKA and M. RĘKAS, *Sensors and Actuators* B **47** (1998) 194.
85. M. RADECKA, PRZEWOŹNIK and K. ZAKRZEWSKA, *Thin Solid Films* **391** (2001) 247.
86. R. MOOS, W. MENESKLOU, H.-J. SCHREINER and K. H. HÄRDTL, *Sensors and Actuators* B **67** (2000) 178.
87. W. MENESKLOU, H. J. SCHREINER, K. H. HÄRDTL and E. IVERS-TIFFÉE, *ibid.* **59** (1999) 184.
88. M. L. POST, J. J. TUNNEY, D. YANG, X. DU and D. L SINGLETON, *ibid.* **59** (1999) 190.
89. L. XUCHEN, X. TINGXIAN and D. ZIANGHONG, *ibid.* **67** (2000) 24.
90. T. S. STEFANIK and H. L. TULLER, *J. Eur. Ceram. Soc.* **21** (2001) 1967.
91. N. IZU, W. SHIN and N. MURAYAMA, *Sensors and Actuators* B **87** (2003) 99.
92. N. IZU, W. SHIN, H. MURAYAMA and S. KANZAKI, *ibid.* **87** (2003) 95.
93. K. KIUKKOLA and C. WAGNER, *J. Electrochem. Soc.* **104**(6) (1957) 379.
94. W. WEPPNER, *Mater. Sci. Eng.* B **15** (1992) 48.
95. N. YAMAZOE and N. MIURA, *J. Electroceram.* **2**(4) (1998) 243.
96. A. DUBBE, *Sensors and Actuators* B **88** (2003) 138.
97. F. H. GARZON, E. L. BROSHA and R. MUKUNDAN, in "Proc. Electrochemical Soc. (High Temperature Materials)," Vol. PV 2002-5, edited by S. Singhal (The Electrochemical Society, Pennington, NJ, 2002) p. 157.
98. T. H. ETSELL and S. N. FLENGAS, *Chem. Rev.* **70**(3) (1970) 339.
99. B. C. H. STEELE, *Mater. Sci. Eng.* B **13** (1992) 79.
100. T. A. RAMANARAYANAN and W. L. WORRELL, *Can. Metall. Quart.* **13**(2) (1974) 325.
101. J. W. PATTERSON, E. C. BOGREN and R. A. RAPP, *J. Electrochem. Soc.* **114**(7) (1967) 752.

102. K. R. SRIDHAR and J. A. BLANCHARD, *Sensors and Actuators* B **59** (1999) 60.
103. W. C. MACKRODT and P. M. WOODROW, *J. Amer. Ceram. Soc.* **69**(3) (1986) 277.
104. A. DWIVEDI and A. N. CORMACK, *Phil. Mag.* A **61**(1) (1990) 1.
105. P. J. BOTHA, J. C. H. CHIANG, J. D. COMINS, P. M. MJWARA and P. E. NGOEPE, *J. Appl. Phys.* **73**(11) (1993) 7268.
106. J. A. KILNER and B. C. H. STEELE, in "Nonstoichiometric Oxides," edited by O. T. Sørensen (Academic Press, New York, NY, 1981) p. 233.
107. J. KONDOH, H. SHIOTA, S. KIKUCHI, Y. TOMII, Y. ITO and K. KAWACHI, *J. Electrochem. Soc*. **149**(2) (2002) J59.
108. J.-H. LEE, S. M. YOON, B.-K. KIM, J. KIM, H.-W. LEE and H.-S. SONG, *Sol. St. Ionics* **144** (2001) 175.
109. K. NOMURA, Y. MIZUTANI, M. KAWAI, Y. NAKAMURA and O. YAMAMOTO, *ibid.* **132** (2000) 235.
110. D. W. STRICKLER and W. G. CARLSON, *J. Amer. Ceram. Soc.* **47**(3) (1964) 122.
111. J. M. DIXON, L. D. LAGRANGE, U. MERTEN, C. F. MILLER and J. T. PORTER, II, *J. Electrochem. Soc.* **110**(4) (1963) 276.
112. J. P. GOFF, W. HAYES, S. HULL, M. T. HUTCHINGS and K. N. CLAUSEN, *Phys. Rev*. B **59**(22) (1999) 14202.
113. A. N. CORMACK, *Mater. Sci. Forum* **7** (1986) 177.
114. C.-K. LOONG, J. W. RICHARDSON, JR., M. OZAWA and M. KIMURA, *J. Alloys and Compounds* **207/208** (1994) 174.
115. C. R. A. CATLOW, A. V. CHADWICK, G. N. GREAVES and L. M. MORONEY, *J. Amer. Ceram. Soc.* **69**(3) (1986) 272.
116. W. L. ROTH, R. WONG, A. I. GOLDMAN, E. CANOVA, Y. H. KAO and B. DUNN, *Sol. St. Ionics* **18/19** (1986) 1115.
117. M. COLE, C. R. A. CATLOW and J. P. DRAGUN, *J. Phys. Chem. Solids* **51**(6) (1990) 507.
118. P. LI, I.-W. CHEN and J. E. PENNER-HAHN, *Phys. Rev*. B **48**(14) (1993) 10074.
119. *Idem.*, *J. Amer. Ceram. Soc.* **77**(1) (1994) 118.
120. M. H. TUILIER, J. DEXPERT-GHYS, H. DEXPERT and P. LAGARDE, *J. Sol. St. Chem.* **69** (1987) 153.
121. A. BOGICEVIC, C. WOLVERTON, G. M. CROSBIE and E. B. STECHEL, *Phys. Rev*. B **64** (2001) 14106-1.
122. A. BOGICEVIC and C. WOLVERTON, *Europhys. Lett*. **56**(3) (2001) 393.
123. F. SHIMOJO, T. OKABE, F. TACHIBANA, M. KOBAYASHI and H. OKAZAKI, *J. Phys. Soc. Jap.* **61**(8) (1992) 2848.
124. X. LI and B. HAFSKJOLD, *J. Phys: Condens. Matter* **7** (1995) 1255.
125. M. O. ZACATA, L. MINERVINI, D. J. BRADFIELD, R. W. GRIMES and K. E. SICKAFUS, *Sol. St. Ionics* **128** (2000) 243.
126. M. S. KHAN, M. S. ISLAM and D. R. BATES, *J. Mater. Chem*. **8**(10) (1998) 2299.
127. R. D. SHANNON, *Acta Cryst*. A **32** (1976) 751.
128. P. J. CHABA and P. E. NGOEPE, in "Mater. Res. Symp. Proc. (Solid-State Chemistry of Inorganic Materials)," Vol. 453, edited by P. K. Davis, A. J. Jacobson, C. C. Torardi and T. A. Vanderah (Mater. Res. Soc., Pittsburgh, PA, 1997) p. 549.
129. H. A. JOHANSEN and J. G. CLEARY, *J. Electrochem. Soc.* **111**(1) (1964) 100.
130. M. OHTA, J. K. WIGMORE, K. NOBUGAI and T. MIYASATO, *Phys. Rev.* B **65** (2002) 174108-1.
131. S. P. S. BADWAL, F. T. CIACCHI and D. MILOSEVIC, *Sol. St. Ionics* **136/137** (2000) 91.
132. Z. WANG, Z. Q. CHEN, S. J. WANG and X. GUO, *J. Mater. Sci. Lett*. **19** (2000) 1275.
133. Z. WANG, Z. Q. CHEN, J. ZHU, S. J. WANG and X. GUO, *Rad. Phys. Chem*. **58** (2000) 697.
134. X. GUO, *Phys. Stat. Sol.* (a) **183**(2) (2001) 261.
135. A. P. SELLARS and B. C. H. STEELE, *Mater. Sci. Forum* **34–36** (1988) 255.
136. D. K. HOHNKE, *J. Phys. Chem. Solids* **41** (1980) 777.
137. L. J. GAUCKLER and K. SASAKI, *Sol. St. Ionics* **75** (1995) 203.
138. A. A. E. HASSAN, N. H. MENZLER, G. BLASS, M. E. ALI, H. P. BUCHKREMER and D. STÖVER, *J. Mater. Sci.* **37** (2002) 3467.
139. H.-Y. LU and S.-Y. CHEN, *ibid*. **27** (1992) 4791.
140. A. J. BURGGRAAF, B. A. BOUKAMP, I. C. VINKE and K. J. DE VRIES, *Adv. Solid-State Chem.* **1** (1989) 259.
141. G. ALBERTI, A. CARBONE and R. PALOMBARI, *Sensors and Actuators* B **86** (2002) 150.
142. B. K. NARAYANAN, S. A. AKBAR and P. K. DUTTA, *ibid.* **87** (2002) 480.
143. J. W. FERGUS, *ibid.* **42** (1997) 119.
144. A. DUTTA, N. KAABBUATHONG, M. L. GRILLI, E. DI BARTOLOMEO and E. TRAVERSA, *J. Electrochem. Soc.* **150**(2) (2003) H33.
145. T. BAK, J. NOWOTNY, M. RĘKAS and C. C. SORRELL, *Sol. St. Ionics* **152/153** (2002) 823.
146. D. J. KUBINSKI, J. H. VISSER, R. E. SOLTIS, M. H. PARSONS, K. E. NIETERING and S. G. EJAKOV, in "Ceramic Transactions (Chemical Sensors for Hostile Environments)," Vol. 130, edited by G. M. Kale, S. A. Akbar and M. Liu (The American Ceramic Society, Westerville, OH, 2002) p. 11.
147. W. CAO, O.K. TAN, J. S. PAN, W. ZHU and C. V. GOPAL REDDY, *Mater. Chem. Phys.* **75** (2002) 67.
148. J. H. KIM and G. M. CHOI, *Sol. St. Ionics* **130** (2000) 157.
149. K. KOBAYASHI, S. YAMAGUCHI, T. HIGUCHI, S. SHIN and Y. IGUCHI, *ibid.* **135** (2000) 643.
150. K. E. SWIDER and W. L. WORRELL, *J. Electrochem. Soc.* **143**(11) (1996) 3706.
151. D. SKARMOUTSOS, A. TSOGA, A. NAOUMIDIS and P. NIKOLOPOULOS, *Sol. St. Ionics* **135** (2000) 439.

Received 28 February
and accepted 9 July 2003